CARDIFF UNIVERSITY
PRIFYSGOL CAERDYDD

ORCA – Online Research @ Cardiff

This is an Open Access document downloaded from ORCA, Cardiff University's institutional repository:https://orca.cardiff.ac.uk/id/eprint/99190/

This is the author's version of a work that was submitted to / accepted for publication.

Citation for final published version:

Mikkelsen, Mark, Singh, Krishna , Brealy, Jennifer, Linden, David and Evans, Christopher John 2016. Quantification of y-aminobutyric acid (GABA) in 1 H MRS volumes composed heterogeneously of grey and white matter. NMR in Biomedicine 29 (11) , pp. 1644-1655. 10.1002/nbm.3622

Publishers page: http://dx.doi.org/10.1002/nbm.3622

Please note:
Changes made as a result of publishing processes such as copy-editing, formatting and page numbers may not be reflected in this version. For the definitive version of this publication, please refer to the published source. You are advised to consult the publisher's version if you wish to cite this paper.

This version is being made available in accordance with publisher policies. See http://orca.cf.ac.uk/policies.html for usage policies. Copyright and moral rights for publications made available in ORCA are retained by the copyright holders.

Quantification of GABA in ^{1}H MRS Volumes Composed Heterogeneously of Grey and White Matter

Mark Mikkelsen[a,b,c*], Krish D. Singh[a], Jennifer A. Brealy[d], David E. J. Linden[a,d] and C. John Evans[a]

[a] Cardiff University Brain Research Imaging Centre (CUBRIC), School of Psychology, Cardiff University, Cardiff, UK
[b] Russell H. Morgan Department of Radiology and Radiological Science, The Johns Hopkins University School of Medicine, Baltimore, MD, USA
[c] F. M. Kirby Research Center for Functional Brain Imaging, Kennedy Krieger Institute, Baltimore, MD, USA
[d] MRC Centre for Neuropsychiatric Genetics and Genomics, Institute of Psychological Medicine and Clinical Neurosciences, School of Medicine, Cardiff University, Cardiff, UK

*Correspondence to: M. Mikkelsen, Russell H. Morgan Department of Radiology and Radiological Science, The Johns Hopkins University School of Medicine, 600 N Wolfe St, Baltimore, MD 21287, USA. E-mail: mmikkel5@jhmi.edu

Running head: GABA Quantification in Heterogeneous Volumes
Keywords: GABA; grey matter; metabolite quantification; MRS; partial volume effects; tissue correction; tissue segmentation; white matter
Word count: 6011

Abbreviations used: AUC, area under the curve; CI, confidence interval; CSF, cerebrospinal fluid; CSI, chemical shift imaging; FSPGR, fast spoiled gradient echo; GABA, γ-aminobutyric acid; GM, grey matter; i.u., institutional units; MEGA-PRESS, Mescher–Garwood point resolved spectroscopy; MM, macromolecule; ROC, receiver operating characteristic; SD, standard deviation; SVS, single voxel spectroscopy; WM, white matter.

Abstract

Quantification of γ-aminobutyric acid (GABA) concentration using localized MRS suffers from partial volume effects related to differences in the intrinsic concentration of GABA in grey matter (GM) and white matter (WM). These differences can be represented as a ratio between intrinsic GABA in GM and WM, r_M. Individual differences in GM tissue volume can therefore potentially drive apparent concentration differences. Here, a quantification method that corrects for these effects is formulated and empirically validated. Quantification using tissue water as an internal concentration reference has previously been described. Partial volume effects attributed to r_M can be accounted for by incorporating into this established method an additional multiplicative correction factor based on measured or literature values of r_M weighted by the proportion of GM and WM within tissue-segmented MRS volumes. Simulations were performed to test the sensitivity of this correction using different assumptions of r_M taken from previous studies. The tissue correction method was then validated by applying it to an independent dataset of in vivo GABA measurements using an empirically measured value of r_M. It is shown that incorrect assumptions of r_M can lead to overcorrection and inflation of GABA concentration measurements quantified in volumes composed predominantly of WM. For the independent dataset, GABA concentration was linearly related to GM tissue volume when only the water signal was corrected for partial volume effects. Performing a full correction that additionally accounts for partial volume effects ascribed to r_M successfully removed this dependency. With appropriate assumption of the ratio of intrinsic GABA concentration in GM and WM, GABA measurements can be corrected for partial volume effects, potentially leading to a reduction in between-participant variance, increased power in statistical tests and better discriminability of true effects.

Introduction

An outstanding problem in the quantification of γ-aminobutyric acid (GABA) concentration is the issue of partial volume effects, which arise from signal detection in MRS volumes composed heterogeneously of grey matter (GM), white matter (WM) and cerebrospinal fluid (CSF). Partial volume effects will lead to differences in apparent GABA concentration (e.g., between two participant groups) that are dependent on differences in voxel tissue content but not necessarily on differences in intrinsic concentrations of GABA. Additionally, accounting for tissue differences may reduce the variability of concentration measurements (1), thereby increasing both the power in statistical analyses and the likelihood of detecting true differences. Partial volume effects also have implications for the signal-to-noise ratio of detected spectral peaks, where variations in tissue content will lead to differences in signal intensity.

Early post-mortem studies have indicated that GABA content is nonuniform across the mammalian cerebrum. Fahn and Côté (2) reported large variability in concentration in rhesus monkeys, with highest GABA levels found in subcortical regions (e.g., basal ganglia) and lowest in pure WM (centrum semiovale). Petroff et al. (3) measured GABA concentration in biopsied rabbit brains, revealing two times greater levels in GM compared to WM. Comparatively higher GABA in GM has also been seen in the monkey brain (4). The use of ^{1}H MRS has also revealed regional differences of in vivo GABA across the brain in rats (5) and humans (6–10).

A number of studies have reported a positive linear dependence of MRS-measured GABA on GM volume, where the amount of GABA in pure GM and pure WM can be estimated by linear regression given sufficient variability in tissue content (11). GABA detection using chemical shift imaging (CSI) has been particularly useful in characterizing this relationship given the large range in fractional GM volume sampled across the acquisition slab. CSI studies have shown two- to eight-fold increases in GABA in GM compared to WM (12–14). Single voxel spectroscopy (SVS) experiments have also shown similar findings within more regionally specific volumes (15–18).

This dependency on GM volume has implications for studies that include systematic differences in fractional GM voxel volume either between experimental groups or across individual participants. For instance, in a hypothetical case one set of GABA measurements has been quantified in predominantly WM voxels (such as where significant atrophy in GM has occurred) and is compared to another dataset from a healthy cohort with no GM atrophy. A

difference will likely be apparent but this may not be due to intrinsic differences in GABA concentration but rather to differences in tissue content between the two cohorts. Confounds will also occur where GABA is correlated with a behavioral measure (e.g., impulsivity) or a functional imaging signal (e.g., the blood oxygenation level dependent response) when these other variables also show a dependency on GM volume. Positive relationships between GABA, GM and some other variable of interest will lead to overestimation of the association between GABA and the variable of interest. In contrast, a negative relationship between GM and a variable of interest will lead to underestimation of the positive association between GABA and this variable. Accounting for heterogeneous tissue content therefore constitutes an important step for accurate quantification of in vivo GABA in MRS studies.

However, a hindrance to the implementation of such an approach is the appropriate assumption of the ratio of intrinsic GABA concentration in GM and WM (r_M). Harris et al. (19) recently introduced a comprehensive tissue correction method that accounts for intrinsic GABA signal differences due to partial volume effects. Crucially, their method relies on assuming the ratio of GABA in GM and WM (i.e., r_M). The effect of various ratios on simulated data was investigated, where an r_M value of 2 was predicted to be the most appropriate. This value was then used to correct in vivo data for voxel tissue content differences across participants, where it did not lead to significantly increased variance in the dataset of tissue-corrected GABA concentration measurements.

Here, a tissue correction method mathematically similar to Harris et al. (19) is formulated. However, a different approach is taken in that the ratio of GABA in GM and WM specific to a given region is empirically estimated in a large reference dataset. In many cases a reference dataset may not be available to research groups and r_M would have to be assumed from the literature. We additionally seek to show how various assumptions of r_M taken from previous studies influence the correction. Therefore, our aims were threefold: Firstly, to estimate r_M in the occipital lobe of a large reference cohort. Secondly, to simulate the impact of assuming r_M from literature values when correcting GABA concentration measurements quantified in tissue-heterogeneous volumes. Thirdly, to validate this tissue correction method by applying it to occipital GABA measurements quantified in an independent cohort. These were derived from both macromolecule (MM) -contaminated and -suppressed acquisitions, such that the tissue correction method could be validated for both types of GABA measurements.

Theory

The NMR signal of a given metabolite is proportional to its molar or molal concentration scaled by constants related to the scanner system and the biochemical sample:

$$S_M = kR_M C_M \quad [1]$$

where S_M is the observed signal of the metabolite of interest, k is a complex global proportionality constant containing numerous system scaling factors (e.g., receive gain, coil loading, pulse sequence design, voxel volume, etc.) and C_M is the metabolite concentration (equal to the number of moles of the molecule). The signal attenuation factor R_M accounts for the transverse and longitudinal relaxation of the metabolite:

$$R_M = \exp\left(-\frac{TE}{T_{2,M}}\right)\left[1 - \exp\left(-\frac{TR}{T_{1,M}}\right)\right] \quad [2]$$

where TE and TR are the echo and repetition times of the acquisition and $T_{1,M}$ and $T_{2,M}$ are the T_1 and T_2 relaxation times of the metabolite. It is assumed that the relaxation times of metabolites do not differ markedly across GM and WM (20–23).

For a given localized spectroscopic voxel, the metabolite concentration will be equal to a weighted sum of the intrinsic concentration of the metabolite in each MR-visible tissue compartment in the brain (11,24). This can be formulated as follows:

$$C_M = \alpha x + \beta y + \gamma z \quad [3]$$

where α, β and γ are the volume fractions of GM, WM and CSF within the voxel and x, y and z represent the basis concentrations of the metabolite in GM, WM and CSF. It is important to note that Eq. [3] assumes that the basis metabolite concentration for each compartment does not change throughout the cerebrum.

GM, WM and CSF volumes in the voxel can be determined by tissue segmentation algorithms available in widely used MRI software packages (e.g., FSL, SPM or FreeSurfer), such that the terms α, β and γ equate to the fractional voxel volumes for each tissue compartment: $\alpha = f_{GM}$, $\beta = f_{WM}$, $\gamma = f_{CSF}$. The basis concentrations can now be represented as: $x = M_{GM}$, $y = M_{WM}$, $z = M_{CSF}$. Rewriting Eq. [1] gives

$$S_M = kR_M(f_{GM}M_{GM} + f_{WM}M_{WM} + f_{CSF}M_{CSF}) \quad [4]$$

The concentration of most metabolites in CSF is negligible (25,26). Therefore, the CSF terms can be removed from the equation. This then requires that the GM and WM voxel volume terms be normalized by the amount of tissue in the voxel. Eq. [4] then becomes

$$S_M = kR_M\left[\frac{f_{GM}M_{GM}}{1-f_{CSF}}(1-f_{CSF}) + \frac{f_{WM}M_{WM}}{1-f_{CSF}}(1-f_{CSF})\right] \quad [5]$$

f_{GM} and f_{WM} are normalized by the volume of tissue in the voxel:

$$t_{GM} = \frac{f_{GM}}{1-f_{CSF}} \quad [6]$$

$$t_{WM} = \frac{f_{WM}}{1-f_{CSF}} \quad [7]$$

where t_{GM} and t_{WM} are the fractional GM and WM volumes per unit tissue volume. We now obtain

$$S_M = kR_M[t_{GM}M_{GM}(1-f_{CSF}) + t_{WM}M_{WM}(1-f_{CSF})] \quad [8]$$

$$S_M = kR_M(t_{GM}M_{GM} + t_{WM}M_{WM})(1-f_{CSF}) \quad [9]$$

Since the tissue volumes are based in terms of GM and WM, the basis concentrations of the metabolite can be interpreted as a ratio of M_{GM} to M_{WM}, as so:

$$r_M = \frac{M_{GM}}{M_{WM}} \quad [10]$$

Eq. [9] can be rewritten giving

$$S_M = kR_M(t_{GM}r_MM_{WM} + t_{WM}M_{WM})(1-f_{CSF}) \quad [11]$$

The basis concentrations are now relative to the concentration of the metabolite in pure WM. Consequently, when $r_M = 1$, $M_{GM} = M_{WM}$.

It is common practice in metabolite quantification to standardize to an internal reference (27,28), the signal of which will also be dependent on the tissue composition of the voxel. In such a case, Eq. [11] is modified to become

$$\frac{S_M}{S_N} = \frac{R_M(t_{GM}r_MM_{WM}+t_{WM}M_{WM})}{R_N(t_{GM}r_NN_{WM}+t_{WM}N_{WM})}(1-f_{CSF}) \quad [12]$$

where k is cancelled out (since the reference signal is detected in the same way as the metabolite of interest) and the N terms refer to the reference, which are treated in the same manner as the M terms.

While the choice of a reference is important for a multitude of reasons, such as for being certain any possible effect of a metabolite of interest is due to the metabolite itself and not the reference, correcting for heterogeneous tissue content adds another layer of complexity. From Eq. [12] it can be seen that assuming inappropriate basis concentrations for either the metabolite of interest or the reference will adversely affect the quantified metabolite concentration. It is useful to frame this potential pitfall by considering the normalization factor needed to correct for

partial volume effects. This is a multiplicative tissue correction factor derived from Eq. [11] and is formulated as follows:

$$T_{corr} = (t_{GM} r_M M_{WM} + t_{WM} M_{WM})^{-1} \quad [13]$$

It is important to make clear that the purpose of this normalization is to scale measured concentrations to the concentration that would have been measured if the voxel in which the signal was detected were 50% GM and 50% WM. Therefore, the basis concentrations M_{GM} and M_{WM} must each be divided by the mean of M_{GM} and M_{WM} when performing this correction. In this way, T_{corr} will equal 1 (i.e., no correction) if $t_{GM} = 0.5$. Figure 1 displays T_{corr} as a function of t_{GM} based on a range of assumptions of r_M. It can be clearly seen that incorrectly assuming a large r_M value will lead to inflation of concentration values measured in voxels composed predominately of WM. Thus, inappropriate assumptions of the ratio of the intrinsic metabolite concentration in GM and WM could significantly bias measurements when there is large variability in fractional voxel volumes across participants or groups.

For relative quantification (referencing to another metabolite), the basis concentrations for the reference typically would be taken from previous studies in the literature. When absolute[1] concentration values are desired, a common method is to use tissue water as an internal concentration reference. The use of tissue water as an internal standard has been described extensively (29–34). The major advantages of water referencing over metabolite referencing include the ability to compare data across sites, high signal-to-noise ratio of the water peak and relative ease of acquisition (28). The observed water signal is not homogenous throughout brain tissue, however; tissue-dependent signal relaxation and water density differences have to be taken into account. Gasparovic et al. (35) have described an absolute quantification method that accounts for the differential density and relaxation times of water in voxels composed of nonuniform proportions of GM, WM and CSF, formulated as follows:

$$C_M = \frac{S_M\left(f_{GM}\rho_{H2O,GM}R_{H2O,GM} + f_{WM}\rho_{H2O,WM}R_{H2O,WM} + f_{CSF}\rho_{H2O,CSF}R_{H2O,CSF}\right)}{S_{H2O}R_M(1-f_{CSF})}\left(\frac{\#H_{H2O}}{\#H_M}\right)C_{H2O} \quad [14]$$

where S_{H2O} is the observed water signal, $\rho_{H2O,y}$ is the relative density of MR-visible water in compartment y, $\#H_{H2O}$ and $\#H_M$ are the number of protons that give rise to the water and

[1] The definition of the term "absolute" in metabolite quantification in MRS is controversial and often ambiguous. In this paper, absolute is used to mean that the signal ratio has been calibrated using an internal standard (some reference compound) with an assumed concentration. Other factors that modulate the signal ratio are also assumed. Concentrations are not expressed in conventional biochemical units (mM or μmol/g) but instead in institutional units (i.u.).

metabolite peaks and C_{H2O} is the molar concentration of water (55,000 mM). The differential longitudinal and transverse relaxation times of water in each tissue compartment are corrected for by the attenuation factor $R_{H2O,y}$ (see Eq. [2]). In similar fashion, the metabolite of interest could be referenced to internal tissue water according to Eq. [12], where the signal ratio is

$$\frac{S_M}{S_{H2O}} = \frac{R_M(t_{GM}r_M M_{WM} + t_{WM}M_{WM})(1-f_{CSF})}{R_{H2O}(f_{GM}H2O_{GM} + f_{WM}H2O_{WM} + f_{CSF}H2O_{CSF})} \quad [15]$$

Finally, the equation can be now rearranged to determine the absolute concentration of the metabolite while additionally accounting for tissue-dependent signal weightings of both the metabolite of interest and the water reference:

$$C_M = \frac{S_M(f_{GM}\rho_{H2O,GM}R_{H2O,GM} + f_{WM}\rho_{H2O,WM}R_{H2O,WM} + f_{CSF}\rho_{H2O,CSF}R_{H2O,CSF})}{S_{H2O}R_M(t_{GM}r_M M_{WM} + t_{WM}M_{WM})(1-f_{CSF})}\left(\frac{\#H_{H2O}}{\#H_M}\right)C_{H2O} \quad [16]$$

Eq. [16] quantifies the concentration of the metabolite of interest corrected for relative water and metabolite signal weightings due to signal relaxation and partial volume effects dependent upon given proportions of GM, WM and CSF in a localized spectroscopic voxel, and is represented in institutional units (i.u.).

Methods

Estimation of GABA in GM and WM

Basis concentrations of GABA in GM and WM in the occipital lobe were estimated in a reference cohort of 95 participants (62 females; 23.98 ± 4.48 years). Participants of this reference cohort took part in a multimodal imaging study, which involved several other MRI and neurophysiological measurements (not reported here) and a detailed psychometric assessment. The study was approved by the research ethics committee of the School of Psychology, Cardiff University, and all participants provided written informed consent. This dataset was collected and analyzed prior to and separately from the present investigation. GABA was measured in the medial occipital lobe using Mescher–Garwood point resolved spectroscopy (MEGA-PRESS) (36) on a 3 T GE Signa HDx scanner (GE Healthcare, Waukesha, WI) at the Cardiff University Brain Research Imaging Centre (CUBRIC). Standard acquisition parameters were used: TE/TR = 68/1800 ms, voxel size = 30 × 30 × 30 mm^3, 332 averages, ON editing pulse = 1.9 ppm, OFF editing pulse = 7.5 ppm. Since the GABA signal detected using this spectral editing technique is contaminated by a co-edited macromolecule (MM) signal (37), GABA concentration measurements are termed GABA+. Eight water-unsuppressed scans were additionally acquired.

Tissue water was used as an internal concentration reference, which was corrected for relative signal contributions from GM, WM and CSF according to Eq. [14]. Signal attenuation and CSF correction factors were also applied to the GABA signal. Tissue volume fractions were calculated within the voxel based on a tissue-segmented high-resolution 1-mm isotropic T_1-weighted fast spoiled gradient-echo (FSPGR) structural image (TE/TI/TR = 3.0/450/7.9 ms). Full details of quantification and voxel co-registration and segmentation procedures are described below. A linear regression analysis was then employed to test the relationship between t_{GM} and GABA+ concentration and to estimate M_{GM} and M_{WM} (11). The uncertainty of the gradient of the linear function was estimated by calculating a 95% confidence interval (CI) for the slope parameter.

Sensitivity Analysis

To evaluate the sensitivity of correcting GABA measurements by applying Eq. [13], we assessed the impact of performing the correction on simulated data using various assumptions of r_M. A dataset of 10,000 randomly generated, normally distributed data points was created such that the data were correlated according to a [GABA+] by t_{GM} linear function. The mean and standard deviation (SD) of each variable and the slope of the best-fit line were based on the empirical data from the reference cohort. The simulated GABA+ measurements were then corrected for partial volume effects based on values of r_M estimated from basis concentrations reported in the literature (Table 1). As this tissue correction method is specifically for MRS measurements, we restricted our selection of basis concentrations to in vivo MRS studies in humans to avoid inherent measurement differences between MRS-measured GABA concentration and GABA concentration quantified though "gold standard" histological or ex vivo methods.

As an alternative assessment of sensitivity, we evaluated how the tissue correction method impacts on classifying individuals into a given disease class based on their measured concentration of GABA. Two datasets were created, a diseased cohort (D^+) and a non-diseased cohort (D^-). For each, 100 normally distributed GABA measurements with corresponding t_{GM} values were generated. D^+ represented hypothetical cases where a clinical diagnosis for a disease had been given and where the mean GABA concentration was (arbitrarily) lower than the mean GABA concentration of D^- (~1.40 vs. ~1.70 i.u.). Two separate scenarios were then simulated. In the first, mean t_{GM} for each cohort was approximately equal (~0.47). This corresponded to a

scenario where a diseased cohort exhibits no concomitant cortical atrophy. In the second scenario, D^+ had a lower mean t_{GM} than D^- (~0.40 vs. ~0.47), thereby simulating disease-related cortical atrophy. For the purposes of this analysis, it was assumed that in both cohorts there was a linear dependence of GABA on t_{GM}, where $r_M \approx 2$. This value was chosen as the assumption of r_M for the tissue correction in both scenarios. To assess the discriminative sensitivity of the GABA measure before and after tissue correction, receiver operating characteristic (ROC) curves were plotted and corresponding areas under the curve (AUC) calculated.

Empirical Validation

In Vivo GABA Detection

In vivo GABA concentration was quantified in an independent cohort of 32 volunteers (17 females; 26.1 ± 3.2 years). This study was approved by the research ethics committee of the School of Psychology, Cardiff University, and all participants provided written informed consent.

A 30 × 30 × 30 mm^3 voxel was positioned medially in the occipital lobe with the ventral face of the voxel aligned with the cerebellar tentorium (Fig. 2a). GABA was detected with two 15-min MEGA-PRESS acquisitions on a 3 T GE Signa HDx scanner at CUBRIC. A standard acquisition (TE = 68 ms) was used where Gaussian editing pulses (16 ms duration) were placed at either 1.9 ppm (ON) or 7.5 ppm (OFF), which leads to an MM-contaminated GABA signal (GABA+). A second acquisition (TE = 80 ms) using the symmetric MM suppression method (38,39) was also employed. Here, the editing pulses (20 ms duration) were placed symmetrically about the 1.7 ppm MM resonance (ON = 1.9 ppm, OFF = 1.5 ppm). The MM resonance is in this way excited equally in both ON and OFF scans, and the co-edited MM resonance, which is present to the same extent in both ON and OFF scans, is absent in the difference spectrum. These concentration measurements are termed GABA'. Other scan parameters for both acquisitions were as follows: TR = 1800 ms, 512 averages, 4096 data points, 5 kHz spectral width. For PRESS localization, the sequence included a 3.6-ms 90° slice-selective sinc excitation pulse (2.4 kHz bandwidth) and two 5.2-ms 180° slice-selective sinc refocusing pulses (1.2 kHz bandwidth). Eight water-unsuppressed scans were acquired in each acquisition from which the water signal acted as an internal concentration reference.

A high-resolution T_1-weighted FSPGR structural image (TE/TI/TR = 3.0/450/7.9 ms, flip angle = 20°, voxel resolution = 1 mm^3, FOV = 256 × 256 × 168 mm^3, matrix size = 256 × 256) was acquired for voxel co-registration and tissue segmentation.

Voxel Co-Registration and Segmentation

MRS voxels were co-registered with the FSPGR image using in-house software created in MATLAB, producing a binary voxel mask in individual structural space. Structural images were segmented into probabilistic partial volume maps corresponding to GM, WM and CSF using the automated segmentation tool FAST (40) in FSL following removal of non-brain tissue using BET (41). Each partial volume map was then multiplied by the binary voxel mask to give probabilistic partial volume voxel maps (Fig. 2). The volume of each tissue compartment was calculated by multiplying the volume of tissue (in voxels) in each partial volume map by the mean partial volume estimate. f_{GM}, f_{WM} and f_{CSF} were then calculated by dividing the voxel volume of each tissue compartment by the sum of the voxel volumes. t_{GM} was calculated by dividing f_{GM} by the sum of f_{GM} and f_{WM}.

GABA Quantification

Spectra were processed and GABA was quantified in Gannet (42) using the software's standard processing steps. Three-hertz exponential line broadening was applied to time-domain data prior to Fourier transformation. The data were automatically corrected for frequency and phase drift using spectral registration (43) and Fourier-transformed into the frequency domain. Using a nonlinear least-squares fitting algorithm, the integral of the GABA signal was calculated by fitting a Gaussian function to the GABA peak in the difference spectrum (Fig. 3). The integral of the water signal was calculated by fitting a Lorentzian-Gaussian function to the water peak in the unsuppressed water spectrum. GABA concentration measurements were then standardized to internal tissue water in three separate ways: (i) by only multiplying the signal ratio of GABA to water (S_M / S_{H2O}) by a global concentration scaling factor ($\#H_{H2O}$ / $\#H_{GABA}$ × C_{H2O}), (ii) by additionally correcting the water signal for tissue-dependent signal relaxation and water density differences according to Eq. [14] or (iii) by performing a full tissue correction where both the water and GABA signals are corrected for partial volume effects according to Eq. [16]. For the quantification of GABA concentration where the GABA signal is detected using spectral editing it is necessary to further correct for the estimated degree of MM contamination and for editing

efficiency (MM / κ). MM is the estimated amount of GABA in the MM-contaminated GABA signal (0.45) and κ is the editing efficiency of GABA-editing (0.5). Note that for the purposes of this study and the sake of consistency the MM correction factor was also applied to the MM-suppressed GABA measurements, meaning that the reported concentration values are approximately half of what would normally be expected. The relative water densities in CSF, GM and WM were assumed to be 1.00, 0.78 and 0.65 (31). The T_1 and T_2 of water were respectively assumed to be 1.33 s and 0.11 s in GM, 0.83 s and 0.08 s in WM (44) and 3.82 s (45) and 0.50 s (46) in CSF. The T_1 and T_2 of GABA were assumed to be 0.80 s and 0.088 s (19). Two protons give rise both to the water peak and the GABA peak. M_{WM} and r_M were estimated from the reference dataset. Given the uncertainty of the regression slope as assessed by the 95% CI, the optimal r_M value was chosen from 100 values calculated by linearly interpolating between the upper and lower bounds of the CI for M_{GM} (at $t_{GM} = 1$). M_{WM} (at $t_{GM} = 0$; i.e., the intercept in the regression model) was kept fixed (see Table 1). The optimal r_M value was that which produced the smallest possible coefficient of determination (R^2) when GABA concentration was regressed against t_{GM} (following correction of the water signal).

Results

Mean ± SD [GABA+] and t_{GM} in the reference cohort was 1.71 ± 0.25 i.u. and 0.47 ± 0.07, respectively. The two variables were significantly linearly related ($R^2 = 0.12$, $p < 0.001$) (Fig. 4), replicating previous findings of a dependency of GABA concentration on GM tissue volume. The slope parameter equaled 1.16, and the 95% CI of this was [0.51, 1.81]. Extrapolating from the regression model, the basis concentrations of GABA in pure GM and WM (M_{GM} and M_{WM}) were estimated to be 2.32 i.u. and 1.16 i.u, respectively ($r_M = 2.00$).

The outcome of the simulated sensitivity analysis is displayed in Figure 5. As expected, the assumption of r_M taken from the reference cohort resulted in the largest reduction in the variance shared by [GABA+] and t_{GM} ($R^2 = 0.001$). This was followed by assumptions of r_M taken from previous empirical studies that estimated a ratio between approximately 1.5 and 3 ($R^2 < 0.03$). Conversely, assumptions of r_M above 6 introduced more shared variance into the regression model ($R^2 > 0.17$). This led to overcorrection, demonstrated by the inflation of GABA measurements in voxels composed predominantly of WM. Correcting for partial volume effects using appropriate assumptions of r_M also reduced the amount of variance within the GABA

dataset (σ^2) compared to the original uncorrected dataset. Overcorrection resulted in increased variance within the GABA dataset.

The ROC curves are plotted in Figure 6. Correcting the GABA measurements when there were no tissue differences between D^+ and D^- led to a small increase in the AUC (0.78 vs. 0.81). This is a result of a decrease in variance within the GABA datasets for both cohorts, which improved discriminative sensitivity. Conversely, the AUC decreased after correction in the scenario where atrophy was simulated in D^+ (0.79 vs. 0.76). Since the tissue correction will raise concentration values measured in predominately WM voxels to remove the tissue dependence (Fig. 1), the overlap in the distributions of the GABA datasets for both cohorts increased, leading to decreased discriminative sensitivity.

Thirty-one pairs of good quality spectra were acquired in the validation experiment. One participant's data were excluded because of a large linewidth as a result of poor B_0 shimming. Mean ± SD [GABA+] was 1.53 ± 0.10 i.u. and mean ± SD [GABA'] was 0.74 ± 0.11 i.u (water tissue-corrected). Tissue segmentation showed an average t_{GM} of 0.41 ± 0.06 across voxels. Regression models of the dependence of GABA concentration on t_{GM} for MM-contaminated and MM-suppressed measurements are displayed in Figure 7. Correcting the water signal alone revealed a linear dependence of [GABA+] on t_{GM} ($R^2 = 0.12$). This dependency was weaker for GABA' ($R^2 = 0.04$). [GABA+] was estimated to be 1.89 i.u. in pure GM and 1.29 i.u. in pure WM ($r_M = 1.47$). For [GABA'], this was 0.97 i.u. in GM and 0.58 i.u. in WM ($r_M = 1.67$).

Performing a full tissue correction led to a substantial reduction in the variance shared between GABA concentration and t_{GM} for both GABA+ and GABA' measurements when compared to only correcting the water signal ($R^2 < 0.001$). The optimal r_M taken from the range of interpolated ratios was 1.45 for GABA+ and 1.57 for GABA'. Additionally, this full correction method did not introduce more variance into the GABA datasets in comparison to the water tissue correction. *F*-tests for equality of variances showed that the variances of the two tissue-corrected datasets were not significantly different from each other for either the GABA+ ($F_{(30, 30)} = 1.05$, $p = 0.90$) or GABA' datasets ($F_{(30, 30)} = 0.97$, $p = 0.93$).

Discussion

The simulations of the sensitivity of correcting for heterogeneous tissue content demonstrate that significant care needs to be taken when assuming the ratio of intrinsic metabolite concentration in GM and WM. An inappropriately large ratio will lead to

overcorrection and introduction of an unwanted negative correlation with fractional GM volume. This would be particularly detrimental for concentrations quantified from data acquired in predominately WM voxels as these values will be greatly inflated. When an appropriate assumption of r_M is used, however, correction for partial volume effects can substantially reduce the variance shared between the quantified metabolite and fractional GM volume, and in principle can decrease the between-participant variance within the metabolite dataset itself. With respect to studies investigating individual or group differences in metabolite levels, appropriately performing a full tissue correction has the benefit of improving the ability to discern true differences by reducing variance of no interest and increasing the power of statistical tests. This conclusion is further supported by the ROC simulations, where the discriminative sensitivity of measured GABA concentration to classify individuals into a given disease class is increased because of reduced between-participant variance in tissue-corrected datasets. Importantly, however, if there are meaningful tissue differences between two cohorts then the tissue correction will rectify overestimation of discriminative sensitivity.

A valid concern is that normalizing GABA measurements as described in this paper may potentially be counterproductive and could increase error, especially if incorrect basis concentrations are assumed. However, tests for equality of variances demonstrated that this additional correction did not add more variance to the GABA datasets. Therefore, we show that correcting GABA concentration for heterogeneous tissue content is a straightforward and viable step in quantification methodology in MRS. This method can be easily applied to other metabolites that are known to exhibit a dependence on GM volume.

Our findings largely mirror the results from Harris et al. (19). The ratio of intrinsic GABA in GM and WM in the occipital lobe was found to be approximately 2 in our reference dataset, which is equal to the ratio the authors recommend for partial volume tissue correction for GABA measurements (r_M is the inverse of what they call α in Eq. (2) in their paper). Our study differs in several key ways, however. Firstly, by having access to a reference dataset with an uncharacteristically large sample size, we were able not only to robustly estimate r_M in a specific region but to also gauge the degree of uncertainty of the slope parameter of the regression model assessing GM tissue volume as a predictor of GABA concentration. We then were able to apply this empirically informed estimation of r_M to correct an independent dataset using a similar MRS acquisition protocol, demonstrating validation of the tissue correction method. Secondly, in our

simulations assessing the sensitivity of the tissue correction, we purposely selected estimations of r_M from previous studies in the literature to highlight explicitly that there are several available empirical sources that can inform on an appropriate (or inappropriate) assumption of r_M. Finally, we acquired MM-suppressed GABA measurements using symmetric MM suppression in addition to GABA+ measurements, and show that the tissue correction method can also be applied to this more specific measure of GABA. These methodological differences from Harris et al.'s investigation corroborate their approach, further validating the use of an assumed ratio of intrinsic GM and WM GABA as a method for accounting for partial volume effects.

To account for the possibility that group or individual differences are attributed to differences in GM volume, it is sometimes usual to treat t_{GM} as a covariate of no interest (e.g., by analysis of covariance or linear regression). Intuitively, this appears to be a sensible approach, given that the aim of an experiment should be to demonstrate that the variance of a dependent variable (e.g., GABA concentration) is mostly explained by the independent variable (e.g., younger vs. older participants) alone, independent of the variance explained by a covariate, such as t_{GM}. However, it is a common mistake to attempt to control for a covariate when the covariate (in this case, t_{GM}) is related to both the dependent and independent variables. Covarying out a covariate that correlates with both of these variables will not just remove some of the unexplained variance, it will also remove variance that would have been attributable to the predicted effect (47). This makes interpreting the outcome of the study problematic and reduces the ability to observe true effects that may otherwise have been evident prior to partialling out the variance attributed to the covariate. The alternative method of normalizing GABA concentration for partial volume effects as presented here obviates this issue as any variance of a covariate shared between GABA concentration and another variable of interest is removed from the GABA measure only. Notably, this approach can be implemented regardless of whether GM volume is associated with GABA and another variable of interest or with GABA alone.

The estimations of the basis concentrations of GABA in GM and WM from previous MRS studies reveal a considerable range in ratios (~1.5–8). This discrepancy is problematic as it adds uncertainty to the appropriate assumption of r_M. It is unclear why such a range of estimations exists, but one possible explanation is that this is down to the variety of spectroscopy techniques that have been employed. The majority have employed SVS, where the exact acquisition approach has included double quantum filtering (15), ultra high-field unedited

spectroscopy (18) and *J*-difference editing (16,17,48). Approaches in CSI experiments have also varied from multiple quantum filtering (14) to 2D *J*-resolved (12) or *J*-difference edited imaging (13). All of these methods have their own advantages and disadvantages with regard to resolving the GABA signal (49), which may play a factor in the inconsistent estimations of M_{GM} and M_{WM}. There is also the problem of different tissue segmentation algorithms and how much they contribute to quantification error. There is already some indication that some of the major toolboxes result in more error than others (35,50). The choice of concentration reference in previous studies is also an important point to consider when explaining the inconsistency of these estimates. Tissue water and creatine are the most commonly used internal references and both require assumptions about their respective intrinsic concentration in the sample prior to conversion to absolute concentration values, adding uncertainty to estimates of basis concentrations. Another plausible explanation is that the sample size in most of these previous investigations has been relatively small (typically three to 10 participants). Even for CSI, where the number of voxels allows for a better estimation of basis concentration across tissue type (at least across brain regions), a small sample size limits the generalisability of estimated basis concentrations. Finally, MM contamination in MEGA-edited spectroscopy will add some variance to the relationship between GABA measurements and GM volume. At least one CSI study has reported a relationship between GM and the MM baseline (51). Indeed, in our independent validation dataset r_M was estimated to be lower for the MM-suppressed measurements compared to the MM-contaminated measurements. Given these discrepancies, we recommend that research groups use reported values of M_{GM} and M_{WM} taken from previous studies that implemented a similar acquisition technique, set of sequence parameters, concentration reference and/or region of interest. Ideally, a reference dataset acquired from a sufficiently large sample at the local research site should be used, but this will not always be possible in some settings.

Aside from the inconsistency in r_M for GABA in the literature, a major limitation with the approach described here is the assumption that this ratio is constant throughout the cerebrum. Given the variation in GABA levels in different cortical and subcortical regions (2,7,10), it is plausible that there are regional differences in the basis concentrations of GABA in GM and WM. Additionally, the correction also assumes that r_M is the same for all individuals, which is unlikely to be the case. To overcome these limitations, r_M would need to be estimated within the

region of interest on a per-participant basis, such as by using CSI. Methodological limitations and time constraints make this impractical, however, particularly in a clinical setting. Alternatively, and as previously stated, a sufficiently large reference dataset that matches the technique and region of interest would circumvent these issues to a certain extent.

Although accounting for differences in the basis concentration of GABA in GM and WM will reduce tissue-dependent signal heterogeneity across participants within a given study, other factors influencing absolute quantification will affect measurements both within and across datasets. For instance, chemical shift displacement artifacts will have an impact on tissue correction procedures given the effective spatial offset of the detected metabolite signal of interest from the nominal voxel from which tissue values are derived. Such signal localization errors will be particularly problematic with PRESS as the slice-selective refocusing pulses typically have relatively low bandwidths and, therefore, suboptimal spatial profiles. To reduce error contributed from these artifacts to tissue correction, the chemical shift displacement of the GABA signal could be determined and tissue values derived from the effective voxel. Relatedly, spatial effects of the MEGA-PRESS experiment will lead to signal loss in particular compartments of localized volumes (52,53), which can only be assessed through numerical simulations or in vitro experiments. In addition, the lineshape of the resolved difference-edited 3.0 ppm GABA multiplet will differ depending on the transition width, refocusing bandwidths and flip angles of the slice-selective refocusing pulses (54). These will differ across acquisition protocol, platform and research site, leading to subtle differences in quantified measures. Finally, it is assumed that the relaxation times of the metabolite of interest are equal or at least similar between GM and WM. Although the in vivo T_1 and T_2 of GABA have been measured previously (19), relaxation differences across tissue type have yet to be characterized and should eventually be taken into account in the absolute quantification procedure. These issues highlight some of the continued difficulties of absolute quantification in MRS, and in particular the absolute quantification of GABA.

A method to correct GABA concentration measurements for partial volume effects in MRS volumes with heterogeneous tissue compositions has been presented and validated. This approach is an extension of an established method that quantifies metabolite concentration using tissue water as an internal reference while correcting for differential water signal contributions across tissue type. Although care must be taken when assuming the basis concentration of

GABA in GM and WM, appropriate assumptions will remove the tissue dependence and could potentially reduce measurement-related variance within the dataset of GABA measurements, enhancing the power of MRS studies of individual differences and pathological changes in neuropsychiatric and neurological disorders.

Acknowledgments

DL and KS were supported by MRC grant MR/K004360/1. The reference cohort study was funded by the National Centre for Mental Health (NCMH) at Cardiff University, with funds from the National Institute for Social Care and Health Research (NISCHR), Welsh Government, Wales (Grant No. BR09). We are grateful to Dr. Lisa Brindley and Peter Hobden for scanning the reference cohort.

References

1. Mato Abad V, Quirós A, García-Álvarez R, Loureiro JP, Álvarez-Linera J, Frank A, Hernández-Tamames JA. The partial volume effect in the quantification of ^{1}H magnetic resonance spectroscopy in Alzheimer's disease and aging. *J Alzheimer's Dis*. 2014;42:801-811. doi:10.3233/JAD-140582.

2. Fahn S, Côté LJ. Regional distribution of γ-aminobutyric acid (GABA) in brain of the rhesus monkey. *J Neurochem*. 1968;15(3):209-213.

3. Petroff OAC, Ogino T, Alger JR. High-resolution proton magnetic resonance spectroscopy of rabbit brain: Regional metabolite levels and postmortem changes. *J Neurochem*. 1988;51(1):163-171. doi:10.1111/j.1471-4159.1988.tb04850.x.

4. Sytinsky IA, Thinh NT. The distribution of γ-aminobutyric acid in the monkey brain during picrotoxin-induced seizures. *J Neurochem*. 1964;11(7):551-556. doi:10.1111/j.1471-4159.1964.tb07506.x.

5. Hong S-T, Balla DZ, Pohmann R. Determination of regional variations and reproducibility in in vivo ^{1}H NMR spectroscopy of the rat brain at 16.4 T. *Magn Reson Med*. 2011;66(1):11-17. doi:10.1002/mrm.22943.

6. Waddell KW, Zanjanipour P, Pradhan S, Xu L, Welch EB, Joers JM, Martin PR, Avison MJ, Gore JC. Anterior cingulate and cerebellar GABA and Glu correlations measured by ^{1}H J-difference spectroscopy. *Magn Reson Imaging*. 2011;29(1):19-24. doi:10.1016/j.mri.2010.07.005.

7. Durst CR, Michael N, Tustison NJ, Patrie JT, Raghavan P, Wintermark M, Sendhil Velan S. Noninvasive evaluation of the regional variations of GABA using magnetic resonance spectroscopy at 3 Tesla. *Magn Reson Imaging*. 2015;33(5):611-617. doi:10.1016/j.mri.2015.02.015.

8. Harada M, Kubo H, Nose A, Nishitani H, Matsuda T. Measurement of variation in the human cerebral GABA level by in vivo MEGA-editing proton MR spectroscopy using a clinical 3 T instrument and its dependence on brain region and the female menstrual cycle. *Hum Brain Mapp*. 2011;32(5):828-833. doi:10.1002/hbm.21086.

9. Veen JW van der, Shen J. Regional difference in GABA levels between medial prefrontal

and occipital cortices. *J Magn Reson Imaging*. 2013;38(3):745-750. doi:10.1002/jmri.24009.

10. Dou W, Palomero-Gallagher N, van Tol M-J, Kaufmann J, Zhong K, Bernstein H-G, Heinze H-J, Speck O, Walter M. Systematic regional variations of GABA, glutamine, and glutamate concentrations follow receptor fingerprints of human cingulate cortex. *J Neurosci*. 2013;33(31):12698-12704. doi:10.1523/JNEUROSCI.1758-13.2013.

11. Hetherington HP, Pan JW, Mason GF, Adams D, Vaughan MJ, Twieg DB, Pohost GM. Quantitative ^{1}H spectroscopic imaging of human brain at 4.1 T using image segmentation. *Magn Reson Med*. 1996;36(1):21-29. doi:10.1002/mrm.1910360106.

12. Jensen JE, de B. Frederick B, Renshaw PF. Grey and white matter GABA level differences in the human brain using two-dimensional, *J*-resolved spectroscopic imaging. *NMR Biomed*. 2005;18(8):570-576. doi:10.1002/nbm.994.

13. Zhu H, Edden RAE, Ouwerkerk R, Barker PB. High resolution spectroscopic imaging of GABA at 3 Tesla. *Magn Reson Med*. 2011;65(3):603-609. doi:10.1002/mrm.22671.

14. Choi I-Y, Lee S-P, Merkle H, Shen J. In vivo detection of gray and white matter differences in GABA concentration in the human brain. *Neuroimage*. 2006;33(1):85-93. doi:10.1016/j.neuroimage.2006.06.016.

15. Choi C, Bhardwaj PP, Kalra S, Casault CA, Yasmin US, Allen PS, Coupland NJ. Measurement of GABA and contaminants in gray and white matter in human brain in vivo. *Magn Reson Med*. 2007;58(1):27-33. doi:10.1002/mrm.21275.

16. Bhattacharyya PK, Phillips MD, Stone LA, Lowe MJ. In vivo magnetic resonance spectroscopy measurement of gray-matter and white-matter gamma-aminobutyric acid concentration in sensorimotor cortex using a motion-controlled MEGA point-resolved spectroscopy sequence. *Magn Reson Imaging*. 2011;29(3):374-379. doi:10.1016/j.mri.2010.10.009.

17. Geramita M, van der Veen JW, Barnett AS, Savostyanova AA, Shen J, Weinberger DR, Marenco S. Reproducibility of prefrontal γ-aminobutyric acid measurements with *J*-edited spectroscopy. *NMR Biomed*. 2011;24(9):1089-1098. doi:10.1002/nbm.1662.

18. Ganji SK, An Z, Banerjee A, Madan A, Hulsey KM, Choi C. Measurement of regional

variation of GABA in the human brain by optimized point-resolved spectroscopy at 7 T in vivo. *NMR Biomed*. 2014;27(10):1167-1175. doi:10.1002/nbm.3170.

19. Harris AD, Puts NAJ, Edden RAE. Tissue correction for GABA-edited MRS: Considerations of voxel composition, tissue segmentation, and tissue relaxations. *J Magn Reson Imaging*. 2015;42(5):1431-1440. doi:10.1002/jmri.24903.

20. Mlynárik V, Gruber S, Moser E. Proton T_1 and T_2 relaxation times of human brain metabolites at 3 Tesla. *NMR Biomed*. 2001;14(5):325-331. doi:10.1002/nbm.713.

21. Ethofer T, Mader I, Seeger U, Helms G, Erb M, Grodd W, Ludolph A, Klose U. Comparison of longitudinal metabolite relaxation times in different regions of the human brain at 1.5 and 3 Tesla. *Magn Reson Med*. 2003;50(6):1296-1301. doi:10.1002/mrm.10640.

22. Träber F, Block W, Lamerichs R, Gieseke J, Schild HH. ^{1}H metabolite relaxation times at 3.0 Tesla: Measurements of T1 and T2 values in normal brain and determination of regional differences in transverse relaxation. *J Magn Reson Imaging*. 2004;19(5):537-545. doi:10.1002/jmri.20053.

23. Choi C, Coupland NJ, Bhardwaj PP, Kalra S, Casault CA, Reid K, Allen PS. T_2 measurement and quantification of glutamate in human brain in vivo. *Magn Reson Med*. 2006;56(5):971-977. doi:10.1002/mrm.21055.

24. Wang Y, Li S-J. Differentiation of metabolic concentrations between gray matter and white matter of human brain by in vivo ^{1}H magnetic resonance spectroscopy. *Magn Reson Med*. 1998;39(1):28-33. doi:10.1002/mrm.1910390107.

25. Glaeser BS, Hare TA. Measurement of GABA in human cerebrospinal fluid. *Biochem Med*. 1975;12(3):274-282. doi:10.1016/0006-2944(75)90129-5.

26. Petroff OAC, Yu RK, Ogino T. High-resolution proton magnetic resonance analysis of human cerebrospinal fluid. *J Neurochem*. 2006;47(4):1270-1276. doi:10.1111/j.1471-4159.1986.tb00750.x.

27. Jansen JFA, Backes WH, Nicolay K, Kooi ME. ^{1}H MR spectroscopy of the brain: Absolute quantification of metabolites. *Radiology*. 2006;240(2):318-332. doi:10.1148/radiol.2402050314.

28. Alger JR. Quantitative proton magnetic resonance spectroscopy and spectroscopic imaging of the brain: A didactic review. *Top Magn Reson Imaging*. 2010;21(2):115-128. doi:10.1097/RMR.0b013e31821e568f.

29. Barker PB, Soher BJ, Blackband SJ, Chatham JC, Mathews VP, Bryan RN. Quantitation of proton NMR spectra of the human brain using tissue water as an internal concentration reference. *NMR Biomed*. 1993;6(1):89-94. doi:10.1002/nbm.1940060114.

30. Christiansen P, Henriksen O, Stubgaard M, Gideon P, Larsson HBW. In vivo quantification of brain metabolites by ^{1}H-MRS using water as an internal standard. *Magn Reson Imaging*. 1993;11(1):107-118. doi:10.1016/0730-725X(93)90418-D.

31. Ernst T, Kreis R, Ross BD. Absolute quantitation of water and metabolites in the human brain. I. Compartments and water. *J Magn Reson Ser B*. 1993;102(1):1-8. doi:10.1006/jmrb.1993.1055.

32. Kreis R, Ernst T, Ross BD. Absolute quantitation of water and metabolites in the human brain. II. Metabolite concentrations. *J Magn Reson Ser B*. 1993;102(1):9-19. doi:10.1006/jmrb.1993.1056.

33. Knight-Scott J, Haley AP, Rossmiller SR, Farace E, Mai VM, Christopher JM, Manning CA, Simnad VI, Siragy HM. Molality as a unit of measure for expressing ^{1}H MRS brain metabolite concentrations in vivo. *Magn Reson Imaging*. 2003;21:787-797. doi:10.1016/S0730-725X(03)00179-6.

34. Gussew A, Erdtel M, Hiepe P, Rzanny R, Reichenbach JR. Absolute quantitation of brain metabolites with respect to heterogeneous tissue compositions in ^{1}H-MR spectroscopic volumes. *Magn Reson Mater Physics, Biol Med*. 2012;25(5):321-333. doi:10.1007/s10334-012-0305-z.

35. Gasparovic C, Song T, Devier D, Bockholt HJ, Caprihan A, Mullins PG, Posse S, Jung RE, Morrison LA. Use of tissue water as a concentration reference for proton spectroscopic imaging. *Magn Reson Med*. 2006;55(6):1219-1226. doi:10.1002/mrm.20901.

36. Mescher M, Merkle H, Kirsch J, Garwood M, Gruetter R. Simultaneous in vivo spectral editing and water suppression. *NMR Biomed*. 1998;11(6):266-272. doi:10.1002/(SICI)1099-1492(199810)11:6<266::AID-NBM530>3.0.CO;2-J.

37. Mullins PG, McGonigle DJ, O'Gorman RL, Puts NAJ, Vidyasagar R, Evans CJ, Cardiff Symposium on MRS of GABA, Edden RAE. Current practice in the use of MEGA-PRESS spectroscopy for the detection of GABA. *Neuroimage*. 2014;86:43-52. doi:10.1016/j.neuroimage.2012.12.004.

38. Henry P-G, Dautry C, Hantraye P, Bloch G. Brain GABA editing without macromolecule contamination. *Magn Reson Med*. 2001;45(3):517-520. doi:10.1002/1522-2594(200103)45:3<517::AID-MRM1068>3.0.CO;2-6.

39. Mikkelsen M, Singh KD, Sumner P, Evans CJ. Comparison of the repeatability of GABA-edited magnetic resonance spectroscopy with and without macromolecule suppression. *Magn Reson Med*. 2016;75(3):946-953. doi:10.1002/mrm.25699.

40. Zhang Y, Brady M, Smith S. Segmentation of brain MR images through a hidden Markov random field model and the expectation-maximization algorithm. *IEEE Trans Med Imaging*. 2001;20(1):45-57. doi:10.1109/42.906424.

41. Smith SM. Fast robust automated brain extraction. *Hum Brain Mapp*. 2002;17(3):143-155. doi:10.1002/hbm.10062.

42. Edden RAE, Puts NAJ, Harris AD, Barker PB, Evans CJ. Gannet: A batch-processing tool for the quantitative analysis of gamma-aminobutyric acid-edited MR spectroscopy spectra. *J Magn Reson Imaging*. 2014;40(6):1445-1452. doi:10.1002/jmri.24478.

43. Near J, Edden R, Evans CJ, Paquin R, Harris A, Jezzard P. Frequency and phase drift correction of magnetic resonance spectroscopy data by spectral registration in the time domain. *Magn Reson Med*. 2015;73(1):44-50. doi:10.1002/mrm.25094.

44. Wansapura JP, Holland SK, Dunn RS, Ball WS. NMR relaxation times in the human brain at 3.0 Tesla. *J Magn Reson Imaging*. 1999;9(4):531-538. doi:10.1002/(SICI)1522-2586(199904)9:4<531::AID-JMRI4>3.0.CO;2-L.

45. Lu H, Nagae-Poetscher LM, Golay X, Lin D, Pomper M, van Zijl PCM. Routine clinical brain MRI sequences for use at 3.0 Tesla. *J Magn Reson Imaging*. 2005;22(1):13-22. doi:10.1002/jmri.20356.

46. Piechnik SK, Evans J, Bary LH, Wise RG, Jezzard P. Functional changes in CSF volume estimated using measurement of water T_2 relaxation. *Magn Reson Med*. 2009;61(3):579-

586. doi:10.1002/mrm.21897.

47. Miller GA, Chapman JP. Misunderstanding analysis of covariance. *J Abnorm Psychol*. 2001;110(1):40-48. doi:10.1037/0021-843X.110.1.40.

48. Evans CJ, Boy F, Edden RA, Singh KD, Sumner P. Regional variations in GABA measured with MEGA-PRESS. In: *Proc. Intl. Soc. Mag. Reson. Med.* Vol 19. ; 2011:3473.

49. Puts NAJ, Edden RAE. In vivo magnetic resonance spectroscopy of GABA: A methodological review. *Prog Nucl Magn Reson Spectrosc*. 2012;60:29-41. doi:10.1016/j.pnmrs.2011.06.001.

50. Klauschen F, Goldman A, Barra V, Meyer-Lindenberg A, Lundervold A. Evaluation of automated brain MR image segmentation and volumetry methods. *Hum Brain Mapp*. 2009;30(4):1310-1327. doi:10.1002/hbm.20599.

51. McLean MA, Barker GJ. Concentrations and magnetization transfer ratios of metabolites in gray and white matter. *Magn Reson Med*. 2006;56(6):1365-1370. doi:10.1002/mrm.21070.

52. Kaiser LG, Young K, Meyerhoff DJ, Mueller SG, Matson GB. A detailed analysis of localized J-difference GABA editing: Theoretical and experimental study at 4T. *NMR Biomed*. 2008;21(1):22-32. doi:10.1002/nbm.1150.

53. Edden RAE, Barker PB. Spatial effects in the detection of γ-aminobutyric acid: Improved sensitivity at high fields using inner volume saturation. *Magn Reson Med*. 2007;58(6):1276-1282. doi:10.1002/mrm.21383.

54. Near J, Evans CJ, Puts NAJ, Barker PB, Edden RAE. *J*-difference editing of gamma-aminobutyric acid (GABA): Simulated and experimental multiplet patterns. *Magn Reson Med*. 2013;70(5):1183-1191. doi:10.1002/mrm.24572.

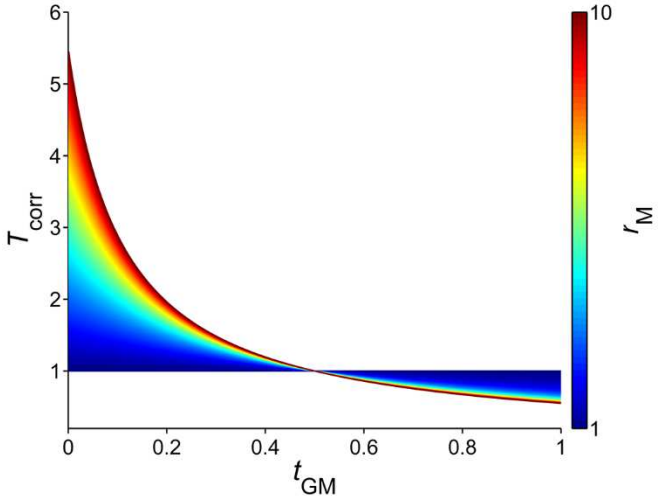

Figure 1. The modelled multiplicative tissue correction factor (T_{corr}) for assumed r_M values ranging from 1 to 10 as a function of fractional GM volume per unit tissue volume (t_{GM}). Assumption of a large r_M necessitates a greater correction for voxels composed predominately of WM, leading to inflation of concentration measurements. The model assumes that the concentration of the metabolite in CSF is negligible, that $f_{CSF} = 0$ and that there are no metabolite relaxation differences between GM and WM.

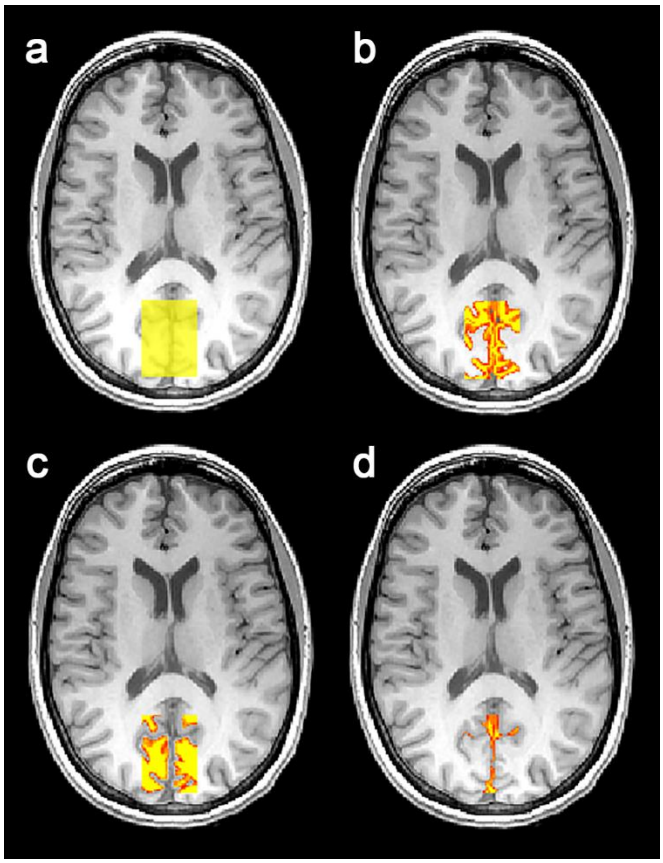

Figure 2. High-resolution T_1-weighted structural image for one participant with the co-registered MRS voxel mask displayed in yellow (a). Corresponding probabilistic partial volume voxel maps following FAST tissue segmentation are shown for GM (b), WM (c) and CSF (d).

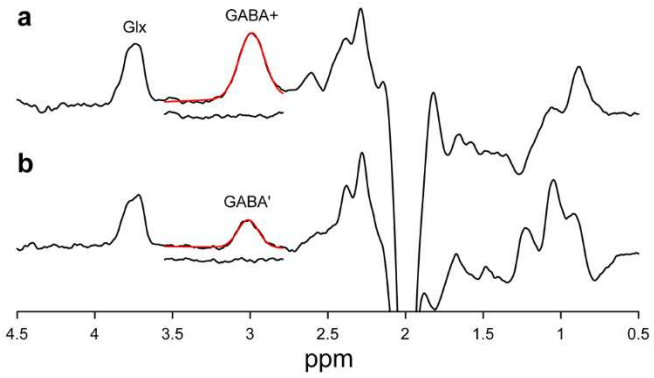

Figure 3. Sample difference spectra from the same participant using standard GABA editing (GABA+) (a) and symmetric MM suppression (GABA') (b). The MM-suppressed spectrum shows a clear reduction in the 3.0 ppm GABA peak amplitude, indicating removal of the co-edited MM signal. Model fits of the Gaussian function to the GABA peak in each spectrum are shown in red. The residuals below each of the fits demonstrate good performance of the fitting procedure.

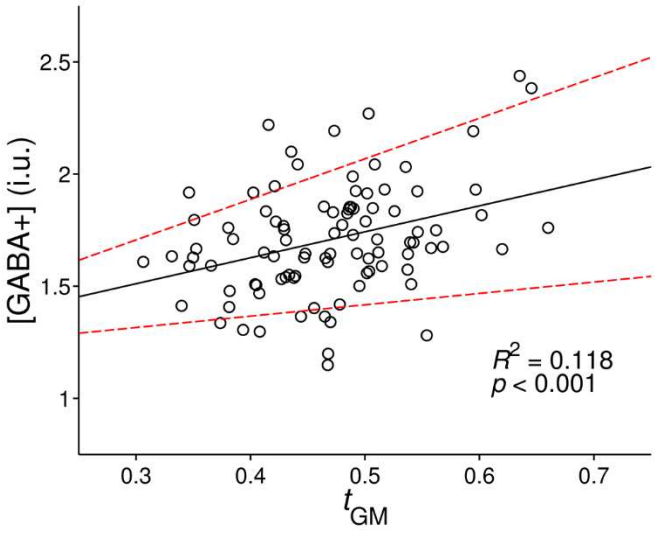

Figure 4. Linear dependence of [GABA+] on t_{GM} in the reference dataset (n = 95). The solid black line is the line of best fit in the linear regression model. The dashed red lines represent the 95% CI for the upper and lower bound of the slope parameter.

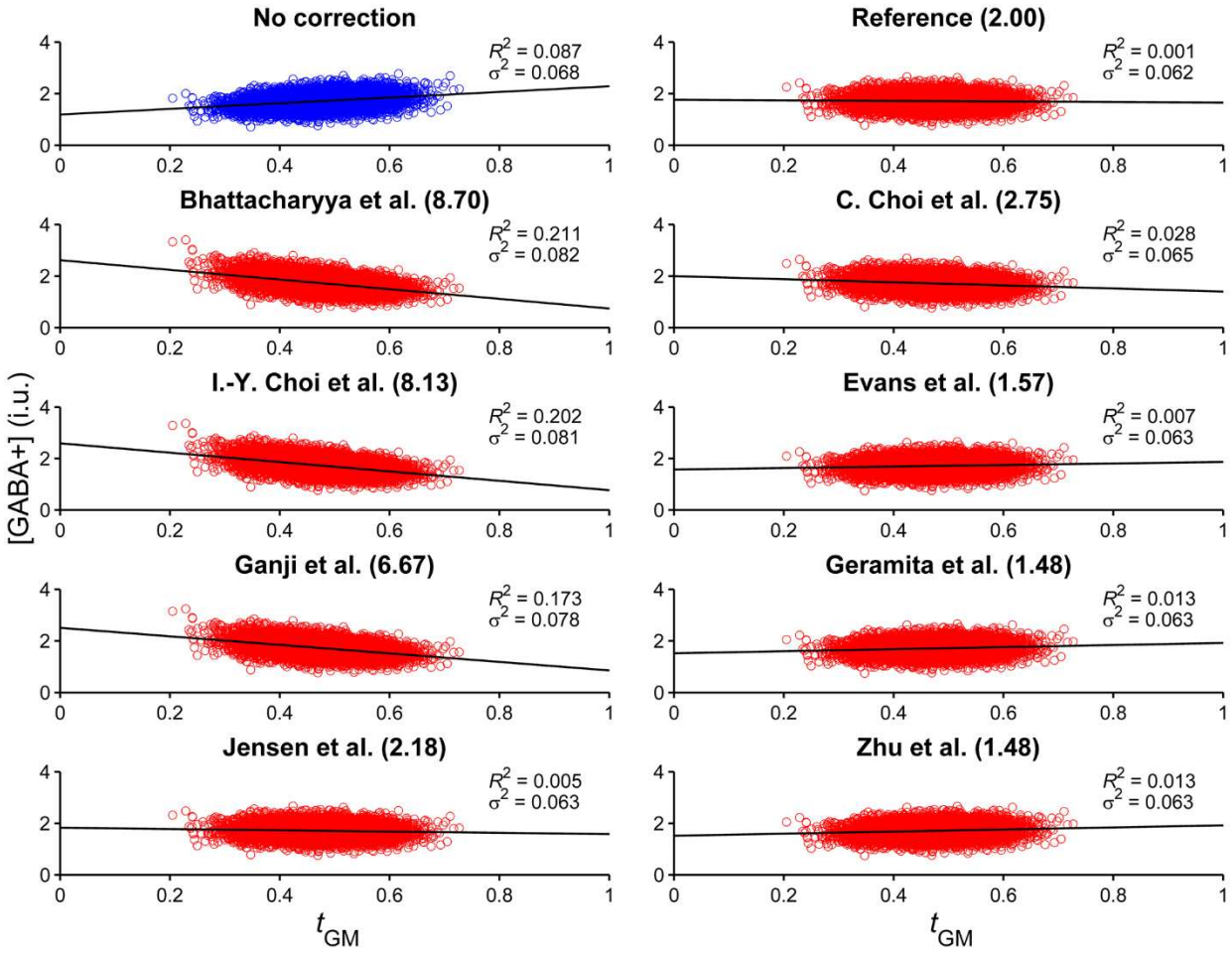

Figure 5. Simulated sensitivity analysis of normalizing the linear dependence of [GABA+] on t_{GM} by assuming various assumptions of r_M (shown in parentheses) estimated from the reference dataset and previous empirical studies. The scatterplot with blue data points shows the uncorrected data while the scatterplots with red data points show corrected data based on each assumption of r_M. The black lines are the lines of best fit in each linear regression model. The coefficient of determination of each model (R^2) and the variance within each simulated GABA dataset (σ^2) are also displayed.

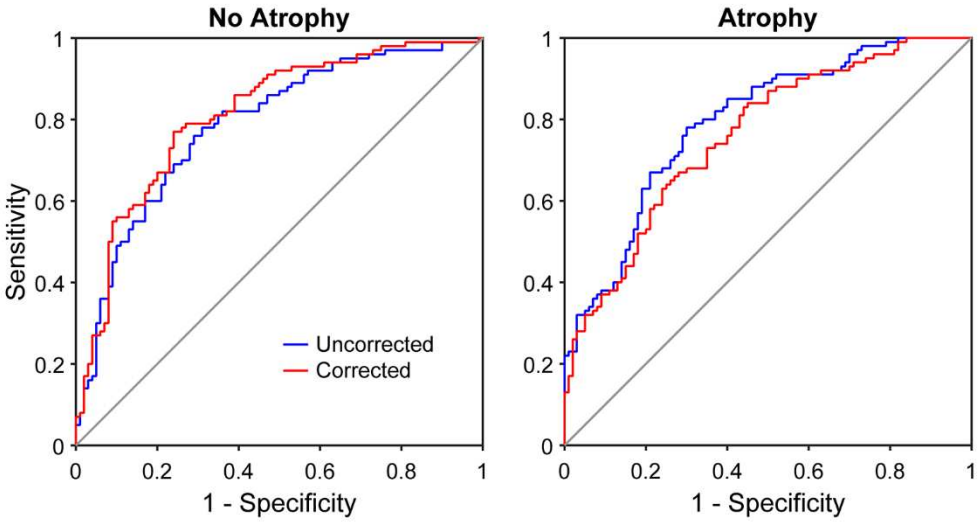

Figure 6. Receiver operating characteristic (ROC) curves illustrating the impact of correcting GABA measurements for tissue-dependent concentration differences in hypothetical diseased (D^+) and non-diseased (D^-) cohorts. Two scenarios were simulated: one where atrophy was not present in D^+ and one where atrophy was present in D^+. The uncorrected ROC curves (blue) in both scenarios had an area under the curve (AUC) of ~0.80. When both cohorts exhibited similar mean t_{GM} values (no atrophy scenario), the tissue correction led to a small increase in the AUC (red ROC curve). When D^+ had a lower mean t_{GM} (atrophy scenario), the tissue correction led to a decrease in the AUC.

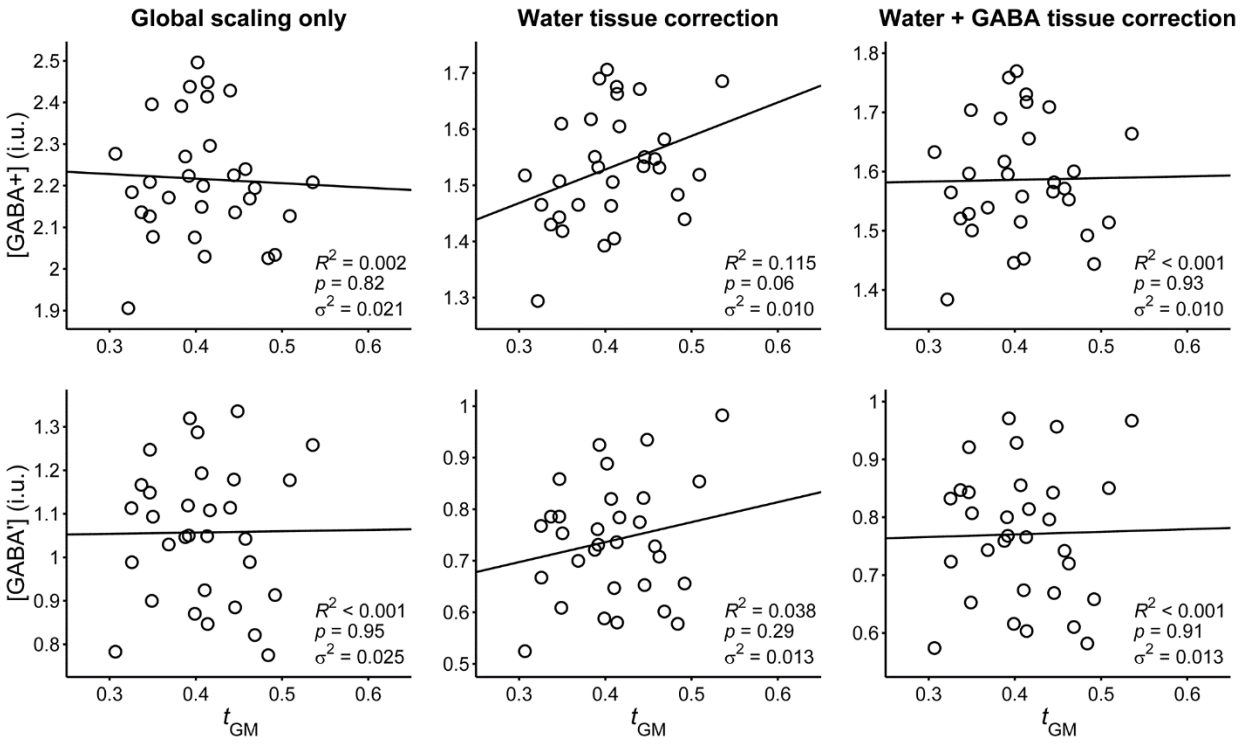

Figure 7. Scatterplots of t_{GM} versus [GABA+] (top row) and versus [GABA'] (bottom row) (n = 31). The leftmost column displays the relationship between t_{GM} and GABA measurements following application of a global concentration scaling factor only. The middle column displays the same relationship following additional tissue correction of the water signal only. The rightmost column shows the relationship when water and GABA are both tissue-corrected. R^2 = coefficient of determination; p = p-value; σ^2 = variance within the GABA dataset.